Saleh Mutashar Hussein ✉
Moharram Jafari
Mohammad Taghi Shervani-Tabar
Seyed Esmail Razavi

NUMERICAL INVESTIGATION INTO PHOTOVOLTAIC (PV) PANEL PERFORMANCE USING A HYBRID NANOFLUID COOLING APPROACH

Summary

Nowadays, photovoltaic (PV) panels are known as effective devices for harnessing solar energy to create healthier and more environmentally friendly energy. However, the operating temperature of a PV system has a significant impact on its efficiency. In this study, a twisted tape was inserted inside a rectangular channel with different values of hybrid nanofluid (1, 2, and 3%) as a coolant fluid to cool the photovoltaic panel for improved efficiency. To stop PV panels from getting too hot, the Ansys Fluent program was used to numerically design a hybrid nanofluid cooling system with 20% MgO and 80% CuO in water as the base fluid. The nanofluids were mixed in different amounts and suspended in water. The impacts of solar radiation (500, 800 and 1,000 W/m^2), and Reynolds numbers on efficiencies were studied. As a result, the average surface temperature (T cell) dropped from 29.16 to 25.87 and the electrical efficiency of the PV modules went up from 11.77% to 11.95% when a 31.25 mm pitch of the twisted tape insert was used inside the rectangular channel at 1,000 W/m^2 of solar radiation. In comparison to a conventional smooth channel, the improved channel significantly lowered the average temperature of the cell by 3.29 °C.

Key words: *sustainable energy; photovoltaic; cell temperature; twisted tape; nanofluid cooling*

1. Introduction

One of the major problems facing the globe now is the need for more energy, particularly as annual energy consumption increases. The issue of energy shortages in many countries may be resolved by using renewable energy, particularly solar energy [1, 2]. Utilising solar energy is an essential tool for addressing urgent issues such as the depletion of fossil fuels, global warming, and the rise in energy demand as a result of modern lifestyle trends. Furthermore, improving energy system performance is another means of achieving sustainability [3, 4]. With the aid of a hybrid photovoltaic thermal system (HPVTS), solar energy may be transformed into usable forms of electrical and thermal energy [5].

Photovoltaic devices are superior to traditional energy sources because they provide humans with renewable, low-cost, and transportable electricity while also being mechanically

durable [6, 7]. A significant problem with current silicon-based PV systems is the degraded performance that comes from using PV panels at temperatures that are still very high. Solar PV panels that are cooled properly have a longer lifespan and less performance degradation [8].

In order to reduce the PV cell working temperature, many studies proposed alternative cooling strategies [9]. The water cooling technique is characterised by high efficiency due to its great capacity and worthy heat transfer coefficient, which improve the conversion efficiency of PV cells [10]. Sheikh at al. introduced a compact and less intrusive forced water cooling system design that can enhance the performance of the PV system by significantly lowering the solar cell working temperature [11]. The cooling method suggested in this paper falls under the active cooling class and it functions via pumping fresh water over a meander-line path that comes into connection with the backsheet PV module.

Sornek et al. created and tested a water cooling system that was specifically designed for solar panels [12]. In order to evaluate how well the cooling system works, two monocrystalline solar panels that are currently on the market were put through tests in a laboratory setting and then in real-world operating settings. The effectiveness and capacity of the PV system were experimentally studied in [13] to see how cooling the PV's rear side of a PV panel affected these properties. The recommended cooling method can be used to efficiently prepare the water supply for a desalination system using reverse osmosis while also being simple and inexpensive. The testing of two identical PV modules, one with cooling and the other without, was done simultaneously.

In [14], a new type of thermal collector for photovoltaic thermal (PVT) systems was suggested. The thermal behaviour of the PV cell and the flow through the cooling box were tied together to make the water-based PVT system efficient at converting heat to electricity and electricity into heat. Under normal operating cell temperature (NOCT) settings, diverse temperatures and inlet mass flow rates were simulated. The use of unwanted air from a centralised system for cooling air is a new method for back cooling presented in this study to make up for the temperature-related reduction in electrical power [15]. The outcomes demonstrated that the wasted air from the system for cooling air is a viable option for back-cooling solar photovoltaic (SPV) panels. Additionally, the calculation of SPV panel performance and the investigation into temperature dispersion are both done using infrared (IR) thermography, along with the identification of surface flaws.

Hudişteanu et al. proposed a mathematical model of PV panels with passive cooling and heat sinks that are perforated and unperforated [16]. The investigation focused on a standard photovoltaic (PV) panel in a stationary location inclined at an angle of 45 degrees with the wind in the direction of its backside. The numerical model base case was calibrated to NOCT conditions using a difficult method. Six backside heat sinks were quantitatively studied. An analysis was done on heat sinks that had perforated and unperforated fins that were horizontal and vertical. In real-world wind conditions, the computational fluid dynamics (CFD) simulation modelled the air volume surrounding the PV panel. Further, an investigation was done into the exergy of a typical thermal PV with air cooling [17]. In order to achieve high efficiency, the mechanical characteristics of efficient performance were determined, namely the length (amount of modules linked in series), intake air temperature, and inlet air flow.

Shrivastava et al. examined how different configurations affect the thermal efficiency of 150-watt PVT collectors [18]. In this PVT system, air-cooling modifications include free ducts with no fins, partially transverse fins, ducts with entirely transverse fins, inclined baffles, and longitudinal fins with straight baffles. The cooling effectiveness was studied using a parametric CFD simulation to estimate the surface and exterior profiles. In [19], glass-to-steel PV panels with 72 monocrystalline solar cells and an overall size of 1,200 millimeters × 540 millimeters were taken into consideration. The PV panel back sheet is comprised of 3 mm mild steel with rectangular fins extending into the collector and 16.26 W/m^2 thermal conductivity. To gather

thermal energy, air is preferably made to flow between thermal collecting devices at a steady speed. In addition to maintaining the PV panel temperature substantially lower than of the typical PVT system, air passing inside the duct also contributes to the relatively higher electrical production of the system.

Hosseinzadeh et al. experimentally explored the effects of using a coolant of 0.2 weight percent ZnO/water nanofluid and a phase change material (PCM) of organic paraffin wax on the thermal and electrical efficiency of a PVT system [20]. Three alternative systems a standard PV module, nanofluid-based PVT system and a PVT/PCM system were investigated and contrasted with one another for this aim. The measured information is examined from an exergy and energy perspective. Siahkamari et al. experimentally enhanced PV module cooling with a novel PCM which absorbs heat from the PV module surface and controls heat capacitance to boost the system efficiency [21]. Cold water with copper microchannel pipes in a chamber at the back of the PV module delays PCM melting. A monocrystalline silicon PV cell has an active area of 26 mm x 30 mm for each matrix. 72 parallel-and-series cells make up the PV module. As a new PCM, sheep fat was used, and 0.004 w/v of CuO nanoparticles were added to boost its cooling effectiveness.

Hassan et al. tested nanofluids (graphene/water) and PCM (RT-35HC) to lower PV system temperatures. This hybrid PVT system was tested against standard PV, PCM, and PV/PCM with water running through pipes inside it [22]. The temperature of the PV, its thermal efficiency, its electrical efficiency, and its overall efficiency were tasted. Sheik et al. carried out an experiment on a PV system that had standard PVs, PCM-cooled PVs, and PVs that used nanophase change material (NPCM) to cool the system to control the temperature of the cells [23]. The PCM was made of polyethylene glycol (PEG) 1000, which could melt at between 33 and 39 degrees Celsius. The insertion materials used were nanomaterials made of alumina and silica.

Sharaf et al. used a passive cooling method containing aluminium metal foam (AMF) with PCM to control the temperature of a PV system [24]. Experiments were carried out in the open air using two different modules: a PV that was not altered in any way and a PV that had AMF integrated in PCM and was designated by the notation PV/PCM/AMF. During the winter season, readings were taken of the distribution of temperature across the PV panel surface, the PCM temperature, the output power produced, and the open-circuit voltage. In [25], outdoor experiments were designed to evaluate the performance of a PVT system that made use of water-based multiwall carbon nanotubes (MWCNT) as a storage of heat and an agent of absorption. While keeping the circulation rate constant at 1.2 litres per minute, an investigation into the influence of changing the volume concentration of nanofluid was carried out within the range of 0%–0.3%.

In [26], a method for cooling a PV panel is proposed that involves the circulation of a nanofluid around the panel. Additionally, it conducts an experimental investigation into the impact of crucial input variables, such as flow rate, ambient temperature, solar radiation, and attributes (output responses) of the nanofluid-cooled HPVTS with respect to nanofluid concentrations, such as exergy loss, overall efficiency, surface temperature, electrical efficiency, and Taguchi's L16 orthogonal array (OA) for generating entropy. It was determined that a Zn-(EG + water) nanofluid including nanoparticle concentrations of 0.1%, 0.3%, 0.5%, and 0.7% was the most effective. The weighting factors for the output answers were calculated with triangular fuzzy numbers (TFN), and the TOPSIS algorithm was used to identify the ideal setting for the input factors. In [27], the analytical hierarchy process (AHP) decision-making was used to systematically compare and contrast the performance of various options for implementing a PV module, such as standalone PV, Al2O3, TiO2, pure water-based, and ZnO-based nanofluid PV/T technologies, and ultimately to select the best option. The best option, as determined by the study, was a PVT system based on the ZnO nanofluid.

Deshmukh et al. studied the properties of a PVT system that was combined with a heat exchanger that had a spiral flow of CuO-water and compared them to those of a PV unit that did not have its temperature lowered [28]. At a constant 0.08 kg/s mass flow rate, the PVT system was built by attaching the heat exchanger to the rear of the polycrystalline PV module.

Rosli et al. studied the effect of using water with different amounts of MWCNT in it ($\theta = 0.3\%$, 0.6%, and 1%) on the performance of a PVT system [29]. Ansys-Fluent was used to study the outlet and the temperature of the PV cell between diverse MWCNT/water nanofluid weight fractions ($\varnothing = 0.3\%$, 0.6%, and 1%) and water with variable fluid inlet velocities between 0.02 and 0.08 m/s.

In a study by Chaichan et al. two alternative PVT systems were practically used to cool a PV module [30]. Water was used to cool one system, while nanofluid and nanoparaffin were used to cool the other. It was decided to use nano-titanium dioxide as an addition to both water and paraffin. The investigation results showed that both water and paraffin thermal conductivity considerably rose with the addition of a 2% mass fraction of nano-TiO2. Prasetyo et al. used TiO2, SiO2, and Al2O3 nanofluids and water heat transfer fluids to model different riser designs on PVT collectors to cool PV solar cells [31]. There were several mass flow rates. The heat transmission process between the fluid and the PV cell layer was simulated using an ANSYS model. Through the use of a stable-state thermal ANSYS model under the simulated controlled settings, only the phenomenon of heat transfer coming from the natural convection of the PV cell layer was taken into account.

In the past five years, twisted tape applications have received a lot of attention in research with the aim of improving heat transfer rates in thermal systems. In [32], an experimental investigation was made to improve the heat transfer rate of the Al2O3 nanofluid with a twisted tape insert inside a U-tube heat exchanger. The coefficients of heat transfer and the corresponding friction factors necessary for performance evaluations were calculated for the heat exchangers under various operating conditions, with particle volume concentrations ranging from 0.01% to 0.03% and twist ratios between 5 and 20. Sowi et al. described the design and analysis of a novel twisted tape with three distinct nanofluids (Al2O3/water, CuO/water, and SiC/water) with a linearly rising/lowering pitch ratio at varied progression rates [33]. For analysis, five alternative twisted tape geometries were considered, including a conventional twisted tape with a constant pitch ratio (PR). The maximum turbulent kinetic energy was produced at the cross-sectional area by the geometry of TT LIPR 0.25 when compared to all other twisted tape geometries.

Experimental proof of the combined effect of the two events was provided in [34]. This method involves using an Al2O3-water nanofluid as the carrier fluid in a pipe that has a variety of twisted tape inserts with varied pitches and twist ratios. A pipe with a stable temperature boundary condition was used to study the impact of nanoparticle volume fractions in the turbulent domain. An analysis of heat transfer enhancement utilising various types of enhanced twisted tape placed in a solar parabolic trough via collectors was reported numerically in [35]. A working fluid with a Reynolds number ranging from 10,000 to 20,000 was pressurised water. Due to the hemisphere insolation from the Sun, it was anticipated that on the solar absorber, the heat flux that was acquired was not uniform.

A six-lobed absorber tube with coupled turbulators was also studied [36]. Hybrid nanoparticles were incorporated into the working fluid to increase the efficiency of the solar unit. A twisted tape and helical coils have been used together. The average solar flux was enforced as the boundary condition for analysing the thermal behaviour and exergy loss. In order to assess the thermal efficiency, which includes the air gap for the solar system, variable heat flux was also used. The effects of altering the working fluid were examined using a homogenous model for hybrid nanomaterials. It was found that a six-lobed tube is preferable to a circular tube because it performs better at cooling and loses less energy.

According to the literature, nanofluids are dispersed mixtures of a cooling fluid and solid nanoparticles. One of the newest techniques for enhancing heat transfer is using nanofluids [37]. Metal oxides, such as aluminium oxide (Al2O3) or cupric oxide (CuO) particles, make up the majority of the used particles. Dispersed particle weight percentages range from 0.1% to 2.0%. Through the cooling fluid, the particles move according to Brownian motion. Greater thermal conductivity and somewhat higher heat capacity are key benefits of nanofluids [38].

A study used the Ansys-Fluent program and the k-ε turbulence model to numerically look at how heat moved from two different model surfaces (the roof and the crown) and how the flow structure changed in the channels with cross-flow-impeding jet flow using water, 0.02% GO (graphene oxide)-water, and 2% diamond-water nanofluids [39]. A ninety-degree-angle fin was added to the upper channel surface at different distances from the impinging jet inlet.

Water and a nanofluid made of 2% CuO were used to measure how heat moves and how fluids flow through a hollow cube and circular models in channels where cross-flow is blocked by jet flow [40]. With the k-ε turbulence model, the Ansys-Fluent tool was used to perform a 3-D steady-state numerical analysis. From the impinging jet intake at D (N) distance, a fin was added to the top channel surface with 45° and 90° angles and D, 1.166 D, and 1.333 D (K) lengths. When the numerical findings from the investigation were compared to the experimental findings in the literature, it was discovered that the results were acceptable and compatible.

The study [41] experimentally investigated the cooling performance of a vehicle radiator using pure water, graphene oxide (GO), and graphene nanoribbon (GNR) nanofluids. Three different fluid inlet temperatures (36, 40, and 44 °C) and four different flow rates (0.6, 0.7, 0.8, and 0.9 m^3 h−1) were performed in the experiments. GO and GNR nanofluids were obtained at 0.01 and 0.02% vol. concentrations by means of pure water as a base fluid. In order to determine the heat transfer enhancement, the experimental data were compared as overall heat transfer coefficients (U) for pure water and nanofluids.

The study [42] examined both numerically and experimentally the convection heat transfer coefficient of a graphene oxide-distilled water nanofluid along a circular copper tube with a constant heat flux at the outside surface under turbulent flow conditions.

In [43], GO (graphene oxide)-distilled water (DW) solutions of volumetric concentrations of 0.01% and 0.02% were numerically analysed in comparison with distilled water in a vertically positioned backward-facing step flow geometry to investigate the heat transfer and flow structures with the turbulence of step corner structures with a chamfer h/2 and h long and without a chamfer. The Ansys-Fluent 18.0 computer program was used to solve conservation equations of a three-dimensional, steady k-ε turbulence model utilising the Boussinesq technique, ultimately yielding the results of the study.

The contribution of this study is development of a numerical PV cooling method using twisted tape inserts inside the duct along with a hybrid nanofluid cooling system (20% MgO, 80% CuO) at different volume concentrations (1, 2, and 3% wt) suspended in water as the base fluid and connected to the back surface of the PV panel to solve the problem of its overheating. This study differs from other studies, firstly, as it uses twisted tape-pitch 31.25 mm inserts inside the channel that create a swirl flow that disrupts the velocity and temperature boundary layers inside the channel, thereby directly increasing the heat transfer coefficient, and secondly, as it uses hybrid nanofluids from 20% MgO and 80% CuO. The proposed methodology consists of designing a PV module with a cooling system using the Ansys-Fluent and SolidWorks programs to clarify the influence of various parameters on the effectiveness of a PV panel. In the boundary conditions used in this study, the fluid inlet boundary temperature remains fixed, but the fluid velocity is variable (0.0015, 0.003, 0.0045, 0.006, 0.009 m/s). Each model tests

three values of input solar energy (500, 800, and 1,000 W/m^2). Solar radiation imposed the input heat flux condition on the panel upper surface.

2. Methodology

The structural cooling system technique is performed based on the flow chart for the approach (Fig. 1).
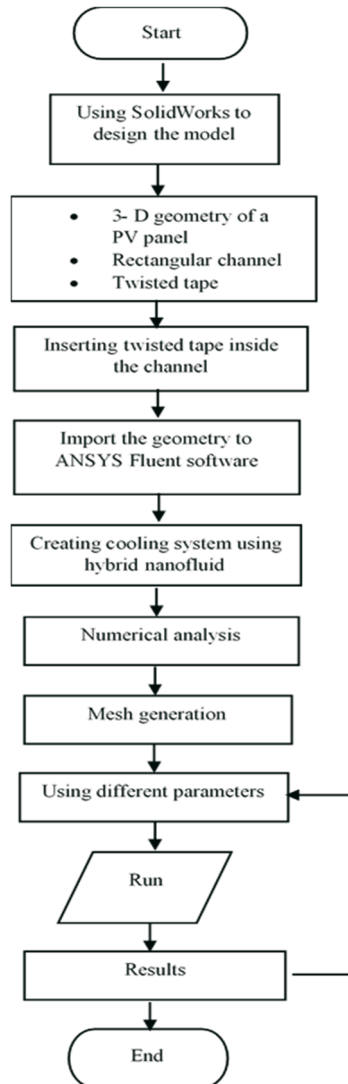
Fig. 1 Design methodology

2.1 Description and assumptions of the model

A three-dimensional PV panel model was built with SolidWorks 2020. According to Fig. 2, the five layers of the PV panel are (from top to bottom): glass, upper ethylene vinyl acetate (EVA) material, PV cells (polysilicon), lower EVA material, and a single layer of tedlar. Thermal paste was used to affix the cooling channel, which was constructed with aluminum metal, to the bottom surface of the PV module. The PV module was insulated to prevent heat loss. The PV panel measured 1,000, 600, and 4.6 mm. Table 1 displays the material properties and layer thickness in the PV panel model.

| Glass |
|---|
| EVA1 |
| Silicon |
| EVA2 |
| Tedlar |
| Thermal paste |
| Aluminium |
| **Water flow** |
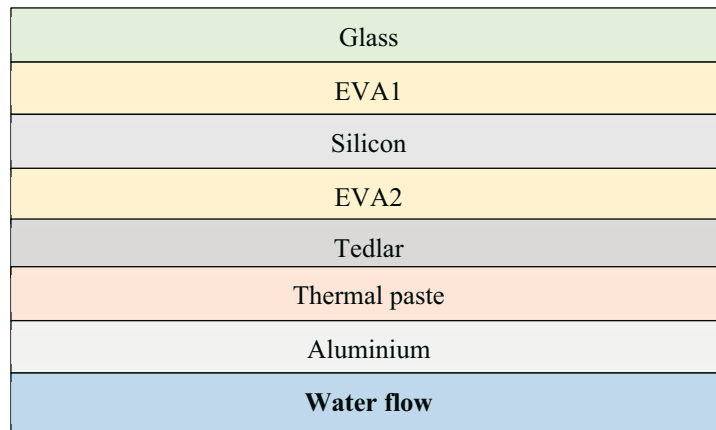
Fig. 2 The physical model of PV panel connected with cooling channel

**Table 1** The material properties and the layer thickness in the PV panel model [**44**]

Materials	Thickness mm	Conductivity W/(m K)	Density kg/m³	Specific heat J/(kg K)
Glass	3	1.8	2,500	500
EVA	0.3	0.311	950	2,090
Silicon	0.5	148	2,329	700
Tedlar	0.1	0.15	1,200	1,250
Thermal paste	0.3	1.9	2,600	700
Aluminium	0.1	237	2,700	903
Water	30	0.6	998.2	41,82

The model consists of two parts:

1- A rectangular channel with dimensions of height, width, and length of 30, 37.5, and 1,000 mm, respectively, was designed using SolidWorks software (Fig. 3).

2- Twisted tape with a 31.25 mm pitch and 25 mm diameter was designed using the SolidWorks software (Fig. 4) and then inserted inside the rectangular channel (Fig. 5). The Ansys-Fluent software (version 2022 R1) was selected to import the geometry from SolidWorks and numerically analyse the results. Hybrid nanofluid entered the domain through the inlet at a temperature of 20 °C and flowed through the outlet.

Fig. 3 Smooth rectangular channel

Diameter of twisted tape (D) (mm)

Pitch (mm)
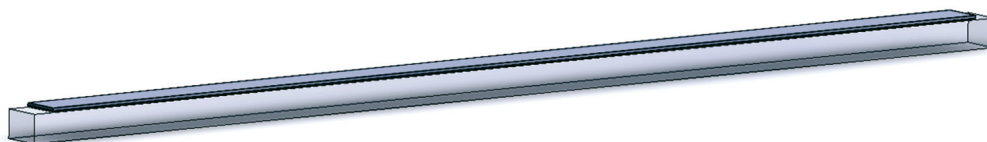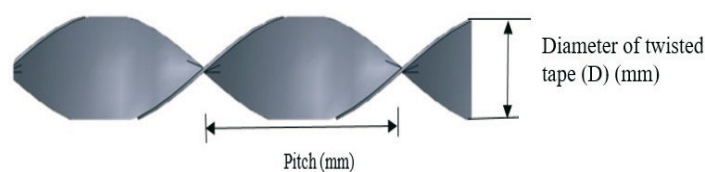
Fig. 4 Twisted tape geometry

Fig. 5 Rectangular channel with pitch of 31.25 mm of twisted tape inserts

To evaluate how effectively the PV modules worked with the new cooling channel, numerical simulations were conducted in Ansys-Fluent, version R 2022. In this steady-state simulation, a number of factors were tested and evaluated, such as Reynolds number (ranging from 50 to 300), solar radiation (500, 800, and 1,000 W/m^2), twisted tape pitch (31.25mm), and rectangular channel shape. With the real-world conditions and component properties in mind, the following assumptions were made to make the simulation go more smoothly:

1. Stable state and incompressible flow.
2. Three-dimensional conjugate heat transfer models for solids and liquids.
3. Constant water velocity and laminar flow.
4. Theoretically, the thermal physical properties of the cooling channel are temperature-independent.
5. No-slip condition.
6. The conduct is ignored.
7. The properties of PV materials remain consistent regardless of the temperature.
8. The side walls are totally protected from the outside world.
9. The transmissivity of the EVA layer is approximately 100%.
10. The temperature of the sky and the landscape are the same.
11. The impact of dusty glass on solar radiation is ignored.

A rectangular channel was used depending on the following parameters (Table 2):

Table 2 PV module parameters

Parameters	values
Solar radiation (W/m^2)	(500, 800, 1,000)
Reynolds number	50, 100, 150, 200, 300
Twisted pitch (mm)	31.25
Twisted length (mm)	1,000
Twisted diameter (mm)	25
Twisted thickness (mm)	1
Temperature inlet ($^\circ$C)	20
Rectangle channel length (mm)	1,000
Rectangle channel width (mm)	37.5
Rectangle channel height (mm)	30
Channels number	16
Efficiency of PV cell under standard test conditions (η_{ref})	12%
Coefficient of heat transfer from glass cover to the surround	5.84 W/(m^2 K)
Type of cooling fluid	hybrid nanofluid
PV material	polysilicon cell
PV length	1000 mm
PV width	600 mm
Reference temperature ($^\circ$C)	25

The inlet velocity was calculated according to the equation below:

$$Re = \frac{\cup_{in} D_h \, \rho}{\mu} \tag{1}$$

where Re denotes the Reynolds number, $\cup_{in}$ denotes the velocity inlet, ρ denotes the density of water, μ denotes the fluid dynamic viscosity (water), and D_h denotes the hydraulic diameter defined as follows:

$$D_h = \frac{4A_f}{P_f} \tag{2}$$

where P_f is the perimeter of the flow channel and A_f is the cross-sectional flow area.

2.2 Governing equations

The conservation equations govern heat transfer and fluid flow in PV cooling [45].
The continuity equation is as follows:

$$\frac{\partial u}{\partial x} + \frac{\partial v}{\partial y} + \frac{\partial w}{\partial z} = 0 \tag{3}$$

Momentum equations are the following:

- in the x direction:

$$\rho u \frac{\partial u}{\partial x} + \rho v \frac{\partial u}{\partial y} + \rho w \frac{\partial u}{\partial z} = -\frac{\partial p}{\partial x} + \mu \left(\frac{\partial^2 u}{\partial x^2} + \frac{\partial^2 u}{\partial y^2} + \frac{\partial^2 u}{\partial z^2} \right) \tag{4}$$

- in the y direction:

$$\rho u \frac{\partial v}{\partial x} + \rho v \frac{\partial v}{\partial y} + \rho w \frac{\partial v}{\partial z} = -\frac{\partial p}{\partial y} + \mu \left(\frac{\partial^2 v}{\partial x^2} + \frac{\partial^2 v}{\partial y^2} + \frac{\partial^2 v}{\partial z^2} \right) + FB + Sy \tag{5}$$

- in the z direction:

$$\rho u \frac{\partial w}{\partial x} + \rho v \frac{\partial w}{\partial y} + \rho w \frac{\partial w}{\partial z} = -\frac{\partial p}{\partial z} + \mu \left(\frac{\partial^2 w}{\partial x^2} + \frac{\partial^2 w}{\partial y^2} + \frac{\partial^2 w}{\partial z^2} \right) \tag{6}$$

where ρ and p are the density and the pressure of the liquid, respectively, and u, v, and w represent the liquid velocities in the x, y, and z orientations, respectively. The Boussinesq approximation states that FB is a buoyancy force, as shown by:

$FB = \rho_O \left(1 - \beta 1 (T - T_O) \right) g$ where T_O and $\beta 1$ are the operation temperature and the thermal expansion coefficient, respectively, and Sy is the body forces $= -\rho \, g \, cos\Theta$.

The energy equation:

A fluid and several solid domains are involved in heat transfer in cooled PV panels. The working fluid in the cooling channel is covered by the fluid domain. For each material layer, a separate solid domain exists (glass, EVA1, 2, PV cells, tedlar, thermal paste, and aluminum) in the PV panel.

The equation below represents the heat transfer for fluids:

$$\rho u \frac{\partial H}{\partial x} + \rho v \frac{\partial H}{\partial y} + \rho w \frac{\partial H}{\partial z} = k \left(\frac{\partial^2 T}{\partial x^2} + \frac{\partial^2 T}{\partial y^2} + \frac{\partial^2 T}{\partial z^2} \right) \tag{7}$$

Furthermore, the heat conduction equation of each solid layer is

$$\rho c p_i \left(\frac{\partial T_i(x,y,z)}{\partial t} \right) = k_i \left(\frac{\partial^2 T_i}{\partial x^2} + \frac{\partial^2 T_i}{\partial y^2} + \frac{\partial^2 T_i}{\partial z^2} \right) + q_i \tag{8}$$

The temperature is represented by T_i, the rate of heat transfer is represented by q_i (W/m³) the layer number is indicated by i, and the fluid thermal conductivity is denoted by the symbol k, and its enthalpy by the symbol H.

2.3 Using hybrid nanofluid as a type of cooling fluid

The use of nanoparticles in water causes the thermal properties of the fluid to differ from those of water. Most studies have focused on metal oxide nanoparticles such as MgO, CuO, Al2O3, ZnO, TiO2, and SiO2 because they are common and not too expensive. CuO nanoparticles were nanoparticles that were crucial in raising the thermal conductivity of traditional cooling solutions Nanofluids have been studied a lot, but some studies showed that spherical nanoparticle nanofluids, such as CuO/nanofluid, do not conduct heat very well like other shapes [46]. In this study, the thermal properties of CuO/nanofluid were improved by using a hybrid nanofluid that contained 20% MgO and 80% CuO nanoparticles mixed with water at different concentrations (1, 2, and 3%). Numerous advantageous qualities exist, including high thermal conductivity resulting from the polyhedral shape of the nanoparticles, low cost, and chemical inertness. Due to its high density and spherical nanoparticle form, CuO has poorer thermal conductivity. The MgO nanoparticles are incorporated into the CuO nanofluid to enhance its thermal characteristics. Hybrid nanofluids are a brand-new class of fluids that were created as a result of the dispersion of a nanoparticle with special features into the nanofluid. Recently, hybrid nanofluids have been utilised due to their potential to facilitate heat transfer. The main thermal characteristics of hybrid nanofluids (density, viscosity, specific heat, and thermal conductivity) are estimated by using equations 9 to 13. As the base fluid (bf) is assumed, the water, nanoparticles (np), and their mixing are the hybrid nanofluids (hnf) [47] (Table 3).

1- Density of the hybrid nanofluid (ρ)

$$\rho_{hnf} = \rho_f \cdot (1 - \emptyset 2)\left((1 - \emptyset 1) + \emptyset 1 \frac{\rho_{s1}}{\rho_f}\right) + \emptyset 2 \rho_{s2} \tag{9}$$

2- Viscosity (μ)

$$\mu_{hnf} = \frac{\mu_f}{(1-\emptyset_1)^{2.5}(1-\emptyset_2)^{2.5}} \tag{10}$$

3- Specific heat (c_p)

$$(\rho c_p)_{hnf} = (\rho c_p)_f (1 - \emptyset_2)\left((1 - \emptyset_1) + \emptyset_1 \frac{(\rho c_p)_{s1}}{(\rho c_p)_f}\right) + \emptyset_2 (\rho c_p)_{s2} \tag{11}$$

4- Thermal conductivity (k)

$$\frac{k_{hnf}}{k_{bf}} = \frac{k_{s2}+(s-1)k_{bf}-(s-1)\emptyset_2(k_{bf}-k_{s2})}{k_{s2}+(s-1)k_{bf}+\emptyset_2(k_{bf}-k_{s2})} \tag{12}$$

where

$$\frac{k_{bf}}{k_f} = \frac{k_{s1}+(s-1)k_f-(s-1)\emptyset_1(k_f-k_{s1})}{k_{s1}+(s-1)k_f+\emptyset_1(k_f-k_{s1})} \tag{13}$$

where (f) is the fluid, (bf) is the base fluid, (hnf) is the hybrid nanofluid, s is the shape factor of nanoparticles = 3, $\emptyset_1$ is the volume fraction of the nanoparticle (CuO), $\emptyset_2$ is the volume fraction of the nanoparticle (MgO), and s1, s2 are nanoparticles of CuO and MgO, respectively.

Table 3 Properties of water, CuO and MgO nanoparticles and hybrid nanofluids

Properties	Water	CuO	MgO	hybrid nanofluid		
				1%	2%	3%
Density (ρ) kg/m^3	998.2	6400	3,580	1,046.49	1,081.59	1,142.556
Viscosity (μ) kg/ (m s)	0.001003			0.001028	0.001054	0.00108
Specific heat (cp) J/ (kg K)	4,182	531	1,030	3,982.17	3,846.33	3,634.86
Thermal conductivity (k) W/(m K)	0.6	19.5	48	0.6167	0.634	0.651

2.4 Computational domain and grid testing

After modelling the PV system and establishing the fluid domain, data analysis was performed using the Ansys-Fluent program. A mesh was created for the geometry design imported from SolidWorks (Fig. 6).
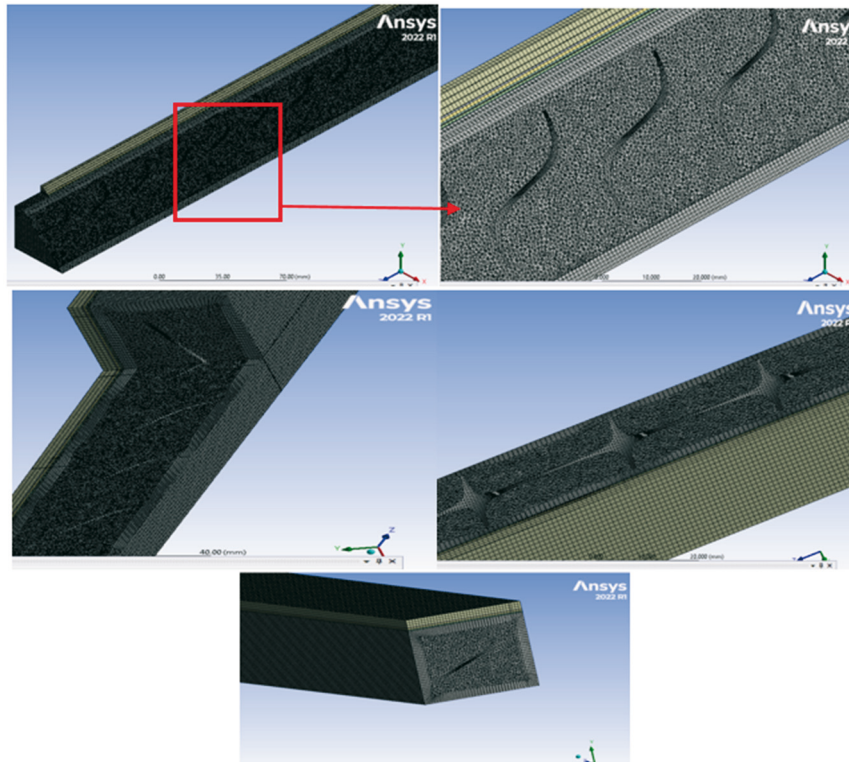
Fig. 6 Mesh generation (rectangular channel)

Using grid testing for the simulation analysis, the accuracy of the simulation results was evaluated. Five alternative grid system were evaluated using the mesh convergence test. The inlet velocity of 0.009 m/s, the ambient temperature of 20 °C, a rectangular channel with a twisted tape pitch of 31.25 mm, and 800 W/m^2 of solar radiation were all used in the mesh convergence test. The temperature of the cell served as the control parameter, and skewness and orthogonal quality were two methods used to evaluate the meshing quality (Fig. 7) [48]. Table 4 displays the grid test results. The differences in the surface temperature (T cell) between the mesh sizes of 8,514,037 and 19,064,173 were barely detectable. The simulation required more processing time and memory, with a mesh size of 19,064,173. Consequently, the numerical investigation used a model with 8,514,037 domain elements.

Skewness mesh metrics spectrum					
Excellent	Very good	Good	Acceptable	bad	Unacceptable
0-0.25	0.25-0.50	0.50-0.80	0.80-0.94	0.95-0.97	0.98-1.00

Orthogonal Quality mesh metrics spectrum					
Unacceptable	Bad	Acceptable	Good	Very good	Excellent
0-0.001	0.001-0.14	0.15-0.20	0.20-0.69	0.70-0.95	0.95-1.00

Fig. 7 Mesh quality recommendations [48]

Table 4 Accuracy of mesh dependency results at solar radiation of 800 W/m², velocity inlet of 0.009 m/s and rectangular channel with twisted tape pitch of 31.25 mm

Element size	Max size	Elements	Average cell temperature (°C)	Time of solution (minute)	Orthogonal quality	Skewness
3 mm	3 mm	641,797	24.78	2	0.70	0.29
2 mm	2 mm	1,354,621	24.60	6	0.74	0.25
1.5 mm	1.5 mm	2,805,051	24.57	12	0.76	0.23
1 mm	1 mm	8,514,037	24.53	83	0.77	0.22
0.75 mm	0.75 mm	19,064,173	24.52	192	0.78	0.21

2.5 The electrical and thermal model for performance evaluation

The electrical efficiency of the PV module is influenced by the temperature of the cell, as shown by the equation below [44]:

$$\eta_{el} = \eta_{ref} \left(1 - \gamma \left(T_c - T_{ref} \right) \right) \tag{14}$$

The reference efficiency of the PV module is given by η_{ref} ($\eta_{ref} = 0.12$); its temperature coefficient is given by γ ($\gamma = 0.0045$ °C $^{-1}$); its temperature of the cell by T_c; and its reference temperature by T_{ref} (25 °C, which is the ideal operating temperature of the PV modules at the predicted power) [39].

E_{in}, is the total solar energy (W/m²), collected by solar cells and given by the equation below:

$$E_{in} = \tau_g \alpha_c G \tag{15}$$

where τ_g is the transmissivity of glass, α_c is the cell absorptivity and G denotes the solar radiation.

The equation below was used to express the electrical energy (W/m²) that the PV cell generated

$$E_{el} = \eta_{el} E_{in} \tag{16}$$

This paper focuses only on the electrical model.

2.6 Boundary conditions

The model names each material component and identifies the regions for each boundary condition. Table 5 symmetrises the inlet temperature of the fluid (20% MgO, 80% CuO, and water as a base fluid) as well as the uniform inlet velocity, fluid outlet, and heat flux generated

at the PV cell. These numbers set the model boundary conditions. In almost all cases, the fluid inlet boundary temperature remains fixed, but the fluid velocity is variable, as indicated in the mentioned table. Each model tests three values of input solar energy. Solar radiation imposed the input heat flux condition on the panel upper surface.

The frame cavity of the simulated model is defined as fluid with a specified speed. The frame sides and the bottom surfaces are defined as adiabatic walls. The convection heat transfer boundary condition is applied at the interface between the PV panel back surfaces and the fluid cooling inside the duct while applying the conduction heat transfer between the corresponding layers. Since the water flow inside the channels is low, the laminar model is selected.

Table 5 The boundary conditions used during simulation

Boundary name	Type	Boundary condition
Inlet boundary condition	Inlet velocity and temperature	U_{in}= 0.0015, 0.003, 0.0045, 0.006 and 0.009 m/sec, T_{in}= 20 °C
Outlet boundary condition	Pressure outlet	at atmospheric pressure 1 atm. ΔP=0
Wall boundary condition	Insulated wall	Vu, Vv, Vw is zero wall heat flux = 0
Upper layer condition	Heat flux	500,800, and 1,000 W/m²

## 2.7   Validation of the model

The validation of the tools used in this research method was carried out against the specimens used is the Ansys- Fluent software version R 2022. This study utilised the numerical results to validate the mathematical model of the PV system [44]. The simulation was set for the PV module with a module area of 0.6 m² and a duct size of 1.0 x 0.6 x 0.03 m (Fig. 8). In the process of validation, the next factors were set: 800 W/m² of solar radiation and a 20 °C ambient air temperature. The rate of mass flow ranged from 0.004 kg/s to 0.018 kg/s. Authors of [44] numerically investigated the influences of the inlet rate of mass flow on the average cell temperature and electrical efficiency of a PV system. As shown in (Fig. 9), the numerical results of this paper [44] and the current study showed excellent concordance, with a standard deviation error of 0.33%-3.78% (Table 6).
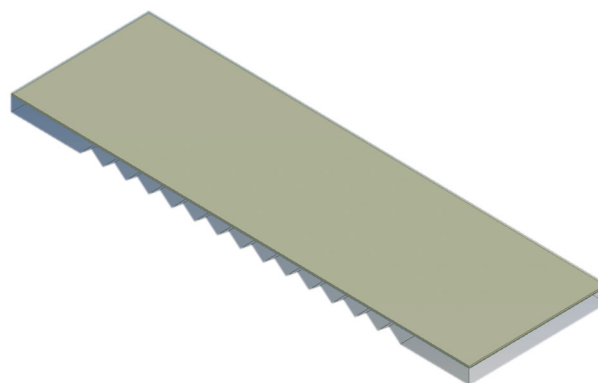
Fig. 8 Special design of cooling channels

S. M. Hussein, M. Jafari,
M. Taghi Shervani-Tabar,
S. Esmail Razavi

Table 6 Error percentage of validation results

Inlet mass flow rate (kg/s)	Cell temperature (°C)		Error
	Present results	Numerical results of [44]	
0.004	37.62	38	1%
0.008	32.61	32.5	0.33%
0.012	30.43	30	1.40%
0.016	29.1	28	3.78%
0.018	28.56	27.5	3.71%
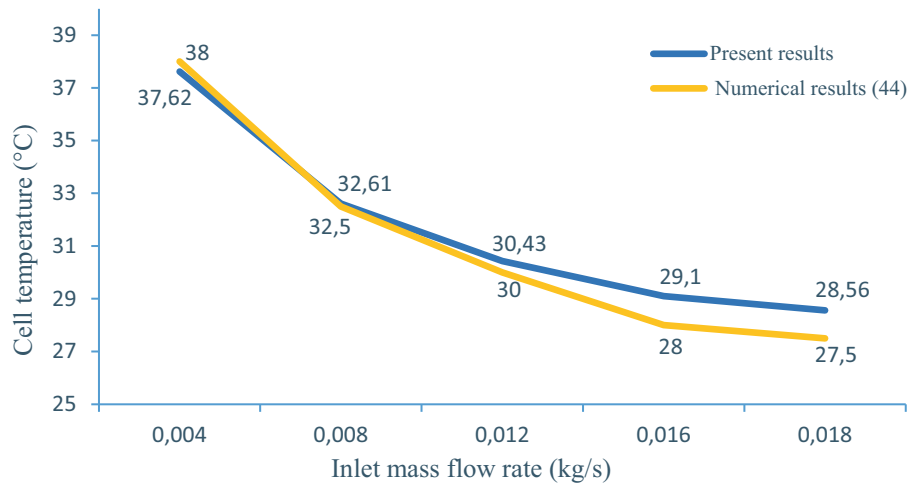
Fig. 9 Effect of the mass flow rate on cell temperature of PV modules (Validation study against data of [44])

3. Results and discussion

The following parameters were used to analyse the PV module performance: twisted tape pitch of 31.25 mm; Reynolds numbers of 50 to 300; solar radiation of 500, 800, and 1,000 W/m^2; and rectangular channel shapes.

The results of using hybrid nanofluids (80% CuO and 20% MgO) are as follows:

3.1 Influence of the twisted tape on the performance of the PV module

The simulations show that adding a twisted tape insert inside the duct with hybrid nanofluids as a coolant fluid can lower the temperature of the cell by 3.29 °C compared to a normal smooth channel, which is shown in Fig. 10 (a, and b). The reduction in average surface temperature (T cell) was from 29.16 to 25.87 °C and an enhancement in the PV module electrical efficiency was from 11.77% to 11.95% when using a 31.25 mm pitch of the twisted tape insert inside the rectangular channel at solar radiation of 1,000 W/m^2 and Reynolds number of 300. Using the twisted tape inside the channel provides a swirl flow that disturbs the speed and temperature boundary layers inside the channel, reducing the cell temperature compared to the smooth rectangular channel. This is also supported by the literature [32].
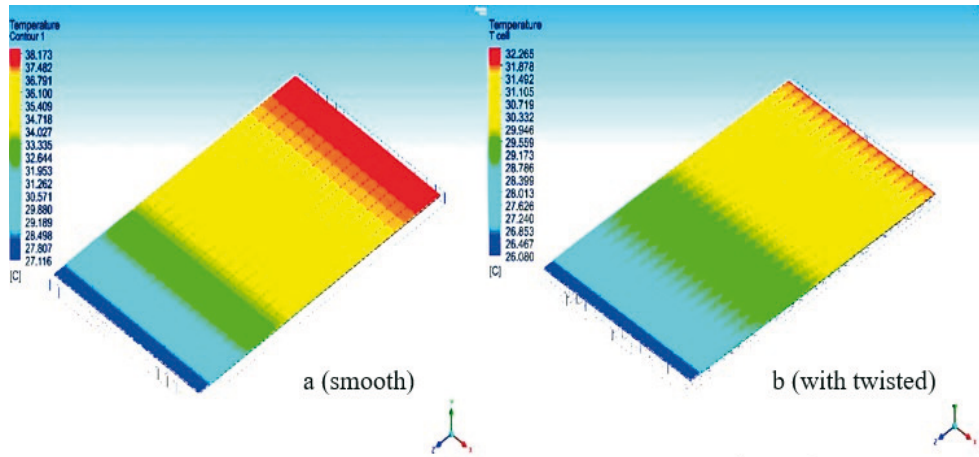
Fig.10 Effect of twisted tape on surface temperature
(**a,** smooth rectangular channel, and **b,** with twisted tape insert)

In contrast, when using different volume concentrations of the hybrid nanofluid (1, 2, and 3%), the average cell temperature is lowered a little bit, as shown in Fig. 11. With solar radiation of 800 W/m2 and Ø 1%, the average cell temperature was 27.77 °C, and it was becoming 27.69 °C and 27.63 °C when Ø = 2% and 3%, respectively.
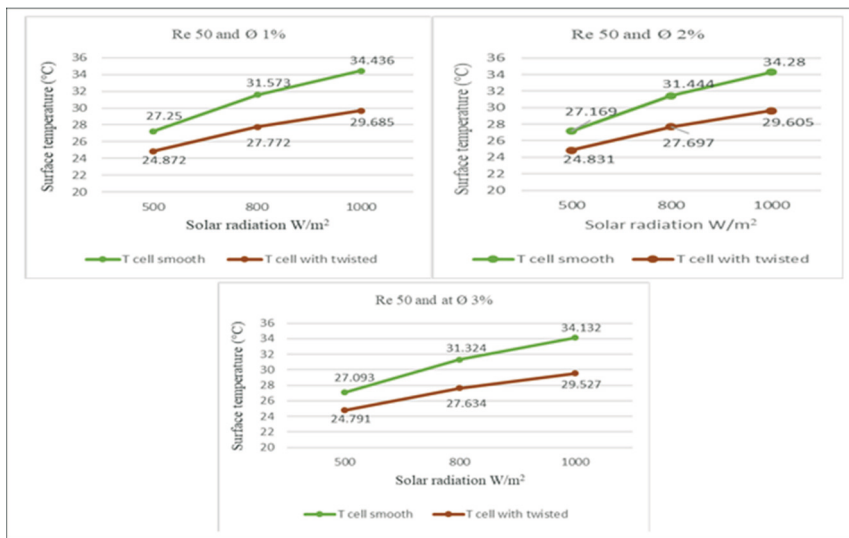
Fig. 11 Influence of the twisted tape on PV performance for diverse volume concentrations of hybrid nanofluid
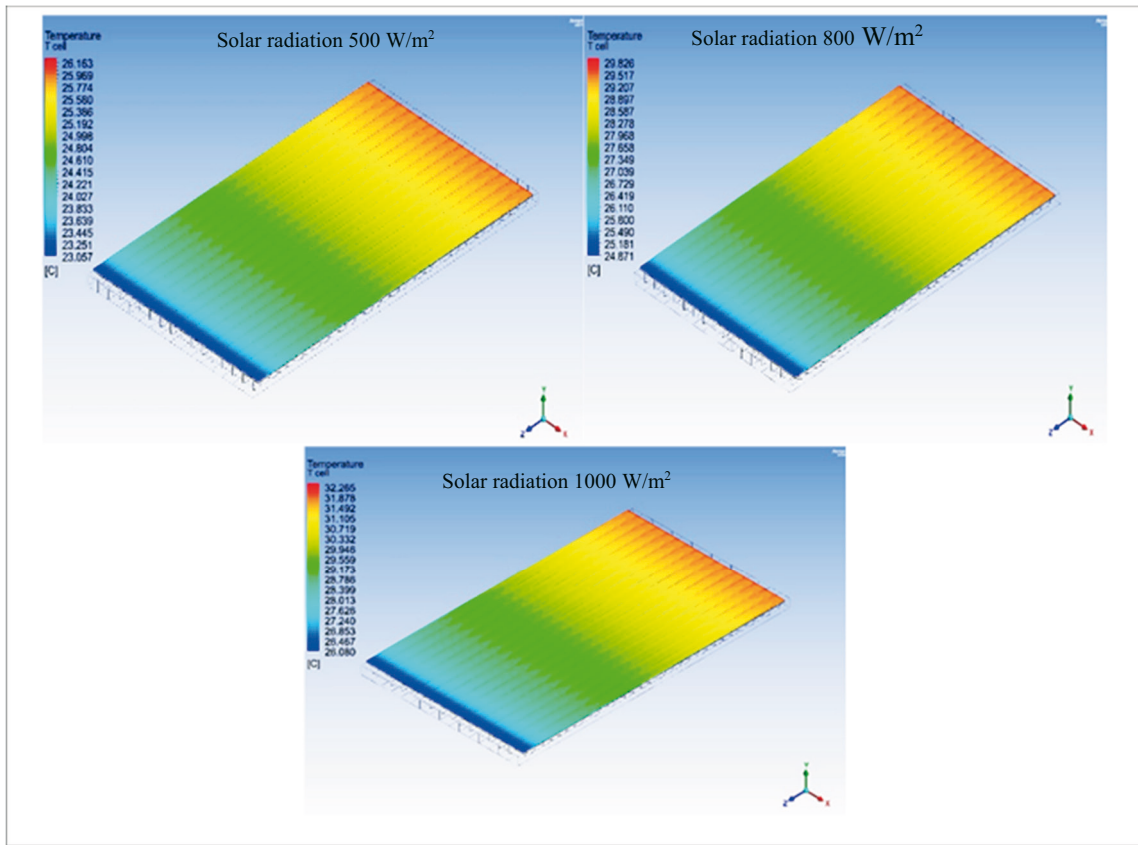
3.2 Impact of solar radiation on the performance of the PV module

Table 7 displays the influence of solar radiation on the surface temperature and the electrical efficiency of the PV modules with different volume concentrations of the hybrid nanofluid for smooth rectangular channels at a velocity inlet of 0.009 m/s. The outcomes obtained show that when solar radiation rose from 500 W/m^2 to 1,000 W/m^2, the average surface temperature (T cell) rose from 24.7°C to 29.39°C, and the electrical efficiency was reduced from 12.016% to 11.76%. In addition, it can also be seen that by increasing the volume concentrations of the hybrid nanofluid, the average cell temperature was lowered and the electrical efficiency increased a little bit. The PV module surface will accumulate more heat as solar radiation increases, leading to an increase in the cell temperature and a decrease in its electric efficiency. The current analysis shows a 0.96 °C surface temperature increases per

100 W/m^2 solar radiation increase, compared to 1.29 °C in [44]. These temperature increases allowed the PV modules with different cooling systems to resist the temperature growth for every 100 W/m^2 increase in solar radiation. The unique cooling channel helped resist the temperature development and maintain the PV module electrical efficiency by lowering the cell temperature.

Table 7 Effects of solar radiation on electrical efficiency and surface temperature of PV modules with different volume concentrations of hybrid nanofluid (smooth rectangular channel).

Solar radiation	Average surface temperature at different volume concentrations (Ø) °C			Electrical efficiency of PV modules with different volume concentrations (Ø) %		
	1%	2%	3%	1%	2%	3%
500	24.7	24.65	24.60	12.01	12.01	12.02
800	27.52	27.44	27.36	11.86	11.86	11.87
1,000	29.39	29.28	29.16	11.76	11.76	11.77

**Fig. 12** The effect of solar radiation on surface temperature (T cell)

Fig. 12 explains the simulation results on how solar irradiation influences the surface temperature. It was observed that by increasing solar radiation, the average cell temperature increased.

3.3 Influence of the Reynolds number on the PV module performance

Fig. 13 shows how the Reynolds number of the cooling fluid affects the cell temperature and electrical efficiency of the PV modules in a rectangular channel with a twisted tape when there is 1,000 W/m^2 of solar radiation. The simulation results show that as the Reynolds number increased from 50 to 300, the average surface temperature (T cell) decreased from 29.68°C to

25.97°C, and the electrical efficiency of the PV modules was increased from 11.74% to 11.94%. In addition, by increasing the volume concentrations of the hybrid nanofluid, the average cell temperature was lowered, and the electrical efficiency improved a little. The swirling motion enhanced the turbulence generator, leading to the blending of the fluid flow. Consequently, the heat transfer coefficient increased in conjunction with the Reynolds number, similar to the findings of [4].
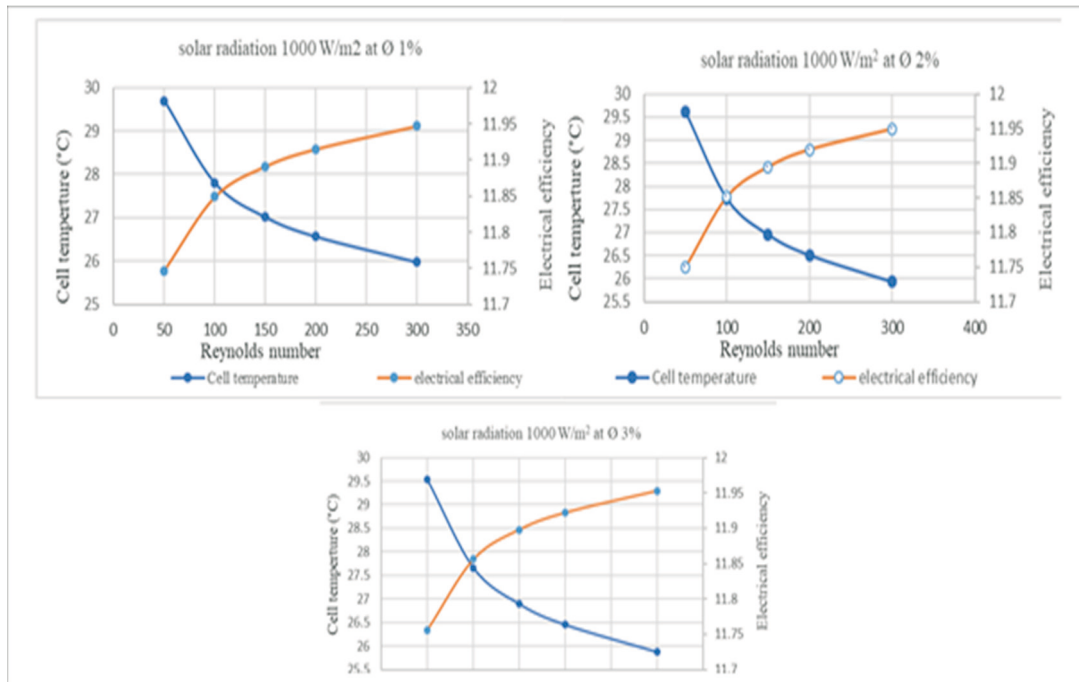

Fig. 13 Effect of Reynolds number of cooling fluid on cell temperature and electrical efficiency of PV modules (rectangular channel with twisted tape)

3.4   Effects of hybrid nanofluid volume concentrations on pressure drops

In Table 8 and Fig. 14, the simulation results show how different amounts of hybrid nanofluid affect pressure drops. The results show that the pressure drops increase with an increase in the Reynolds number and slightly increase with an increase in the hybrid nanofluid volume concentration.

Table 8 Simulation results of effect volume concentrations of hybrid nanofluid on pressure drops

Re	Pressure drops at different volume concentrations (Ø) (Pa)		
	1%	2%	3%
50	0.19	0.2	0.21
100	0.44	0.45	0.46
150	0.72	0.74	0.76
200	1.02	1.05	1.09
300	1.71	1.76	1.8
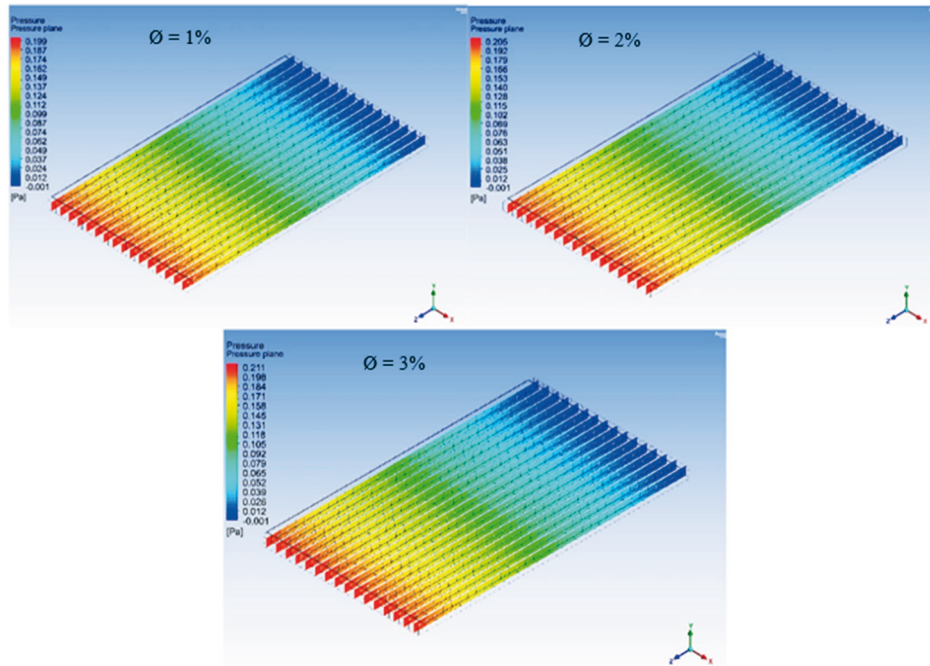
Fig. 14 Effect volume concentrations of hybrid nanofluid on pressure drops
at solar radiation 500 W/m² and Re = 50

4. Conclusion

PV panels are now recognized as efficient tools for capturing solar energy to create cleaner, more sustainable energy. However, the operating temperature of the PV system has an important influence on its efficiency. In this study, twisted tape inserts inside the rectangular channel with varying values of hybrid nanofluid (1, 2, and 3%) were used as a type of coolant fluid to cool the PV panel to increase efficiency. To solve the problem of PV panels getting too hot, Ansys Fluent software was used to build a hybrid nanofluid cooling system with 80% CuO and 20% MgO at different volume concentrations suspended in water as the base fluid. Besides that, the influence of solar radiation and Reynolds number on PV efficiency was studied. According to the simulation findings, the following conclusions were reached:

1) At Reynolds number 50, solar radiation of 800 W/m², and volume concentrations of hybrid nanofluids of 3%, the cell temperature of the smooth channel was 31.32 °C, and it decreased to 27.63 °C when a twisted tape was inserted. Consequently, compared to an ordinary smooth channel, adding a twisted tape insert inside the duct can lower the cell temperature by 3.69 °C.

2) Increasing the volume concentration of the hybrid nanofluid results in a slight decrease in the average cell temperature and an increase in electrical efficiency. It was observed that at solar radiation of 800 W/m² and volume concentrations of hybrid nanofluids of 1%, the average cell temperature was 27.52 °C, and it decreased to 27.44°C when the volume concentration of hybrid nanofluids was 2%.

3) As the solar radiation increased, the average cell temperature increased, and the electrical efficiency decreased. It was observed that when solar radiation increased from 500 W/m² to 1,000 W/m², the average surface temperature (T cell) rose from 24.7°C to 29.39°C, and the electrical efficiency decreased from 12.01% to 11.76%.

4) As the Reynolds number increased, the average cell temperature decreased, and the PV module electrical efficiency improved. It was observed that when the Reynolds number increased from 50 to 300, the average surface temperature decreased from 29.68°C to 25.97°C, and the electrical efficiency of the PV modules increased from 11.74% to 11.94%.

5) The pressure drops rise as the Reynolds number rises and slightly rise when the hybrid nanofluid volume concentration rises. It was observed that when the Reynolds number increased from 50 to 300, the pressure drops increased from 0.19 to 1.71 Pa.

REFERENCES

[1] Abd-Elhady, M. S., Z. Serag, and H. A. Kandil. "An innovative solution to the overheating problem of PV panels." Energy conversion and management **2018**, 157, 452-459. https://doi.org/10.1016/j.enconman.2017.12.017

[2] [Rubbi F, Habib K, Saidur R, Aslfattahi N, Yahya SM, Das L. Performance optimization of a hybrid PV/T solar system using Soybean oil/MXene nanofluids as A new class of heat transfer fluids. Solar Energy. **2020**, 208, 124-38. https://doi.org/10.1016/j.solener.2020.07.060

[3] [Kasaeian A, Bellos E, Shamaeizadeh A, Tzivanidis C. Solar-driven polygeneration systems: Recent progress and outlook. Applied Energy. **2020,** 264,114764. https://doi.org/10.1016/j.apenergy.2020.114764

[4] Yelmen B, Çakır MT, Ün Ç. Estimation of Average Monthly Total Solar Radiation on a Horizontal Surface for the Central Anatolia Region: Example of Sivas Province. Transactions of FAMENA. **2022**, 46(2):1-4. https://doi.org/10.21278/TOF.462028121

[5] Qeays IA, Yahya SM, Asjad M, Khan ZA. Multi-performance optimization of nanofluid cooled hybrid photovoltaic thermal system using fuzzy integrated methodology. Journal of Cleaner Production. **2020**, 256, 120451. https://doi.org/10.1016/j.jclepro.2020.120451

[6] Hashemi SA, Ramakrishna S, Aberle AG. Recent progress in flexible–wearable solar cells for self-powered electronic devices. Energy & Environmental Science. **2020**, 13(3), 685-743. https://doi.org/10.1039/C9EE03046H

[7] Bayat MM, Buyruk E, Can A. Experimental Investigation of PV Panel Performance by Using PCM with Different Fin Geometries. Transactions of FAMENA. **2023**, 47(4):97-108. https://doi.org/10.21278/TOF.474056223

[8] Marinić-Kragić I, Nižetić S, Grubišić-Čabo F, Čoko D. Analysis and optimization of passive cooling approach for free-standing photovoltaic panel: Introduction of slits. Energy Conversion and Management. **2020**, 204, 112277. https://doi.org/10.1016/j.enconman.2019.112277

[9] Benato A, Stoppato A. An experimental investigation of a novel low-cost photovoltaic panel active cooling system. Energies. **2019**, 12(8), 1448. https://doi.org/10.3390/en12081448

[10] Noxpanco MG, Wilkins J, Riffat S. A review of the recent development of photovoltaic/thermal (Pv/t) systems and their applications. Future Cities and Environment. **2020**, 6, 9-9. https://doi.org/10.5334/fce.97

[11] Sheikh YA, Butt AD, Paracha KN, Awan AB, Bhatti AR, Zubair M. An improved cooling system design to enhance energy efficiency of floating photovoltaic systems. Journal of Renewable and Sustainable Energy. **2020**, 12(5), 053502. https://doi.org/10.1063/5.0014181

[12] Sornek K, Goryl W, Figaj R, Dąbrowska G, Brezdeń J. Development and tests of the water cooling system dedicated to photovoltaic panels. Energies. **2022**, 15(16), 5884. https://doi.org/10.3390/en15165884

[13] Shalaby SM, Elfakharany MK, Moharram BM, Abosheiasha HF. Experimental study on the performance of PV with water cooling. Energy Reports. **2022**, 8, 957-61. https://doi.org/10.1016/j.egyr.2021.11.155

[14] Yildirim MA, Cebula A, Sułowicz M. A cooling design for photovoltaic panels–Water-based PV/T system. Energy. **2022**, 256, 124654. https://doi.org/10.1016/j.energy.2022.124654

[15] Ahmad FF, Ghenai C, Hamid AK, Rejeb O, Bettayeb M. Performance enhancement and infra-red (IR) thermography of solar photovoltaic panel using back cooling from the waste air of building centralized air conditioning system. Case Studies in Thermal Engineering. **2021**, 24, 100840. https://doi.org/10.1016/j.csite.2021.100840

[16] Hudișteanu SV, Țurcanu FE, Chereches NC, Popovici CG, Verdeș M, Huditeanu I. Enhancement of PV panel power production by passive cooling using heat sinks with perforated fins. Applied Sciences. **2021**, 11(23), 11323. https://doi.org/10.3390/app112311323

[17] Alayi R, Jahanbin F, Aybar HŞ, Sharifpur M, Khalilpoor N. Investigation of the effect of physical factors on exergy efficiency of a photovoltaic thermal (PV/T) with air cooling. International Journal of Photoenergy. **2022**, 2022, 9882195. https://doi.org/10.1155/2022/9882195

[18] Shrivastava A, Jose JP, Borole YD, Saravanakumar R, Sharifpur M, Harasi H, Razak RA, Afzal A. A study on the effects of forced air-cooling enhancements on a 150 W solar photovoltaic thermal collector for green cities. Sustainable Energy Technologies and Assessments. **2022**, 49, 101782. https://doi.org/10.1016/j.seta.2021.101782

[19] Agrawal Y, Mishra A, Gautam A, Phaldessai G, Yadav AS, Vyas M. Performance analysis of photovoltaic thermal air collector having rectangular fins. Materials Today: Proceedings. **2023**, 84, 6-15. https://doi.org/10.1016/j.matpr.2023.03.787

[20] Hosseinzadeh M, Sardarabadi M, Passandideh-Fard M. Energy and exergy analysis of nanofluid based photovoltaic thermal system integrated with phase change material. Energy. **2018**, 147, 636-47. https://doi.org/10.1016/j.energy.2018.01.073

[21] Siahkamari L, Rahimi M, Azimi N, Banibayat M. Experimental investigation on using a novel phase change material (PCM) in micro structure photovoltaic cooling system. International Communications in Heat and Mass Transfer. **2019**, 100, 60-6. https://doi.org/10.1016/j.icheatmasstransfer.2018.12.020

[22] Hassan A, Wahab A, Qasim MA, Janjua MM, Ali MA, Ali HM, Jadoon TR, Ali E, Raza A, Javaid N. Thermal management and uniform temperature regulation of photovoltaic modules using hybrid phase change materials-nanofluids system. Renewable Energy. **2020**, 145, 282-93. https://doi.org/10.1016/j.renene.2019.05.130

[23] Sheik MA, Aravindan MK, Beemkumar N, Chaurasiya PK, Jilte R, Shaik S, Afzal A. Investigation on the thermal management of solar photo voltaic cells cooled by phase change material. Journal of Energy Storage. **2022**, 52, 104914. https://doi.org/10.1016/j.est.2022.104914

[24] Sharaf M, Huzayyin AS, Yousef MS. Performance enhancement of photovoltaic cells using phase change material (PCM) in winter. Alexandria Engineering Journal. **2022**, 61(6), 4229-39. https://doi.org/10.1016/j.aej.2021.09.044

[25] Abdallah SR, Saidani-Scott H, Abdellatif OE. Performance analysis for hybrid PV/T system using low concentration MWCNT (water-based) nanofluid. Solar Energy. **2019**, 181, 108-15. https://doi.org/10.1016/j.solener.2019.01.088

[26] Qeays IA, Yahya SM, Asjad M, Khan ZA. Multi-performance optimization of nanofluid cooled hybrid photovoltaic thermal system using fuzzy integrated methodology. Journal of Cleaner Production. **2020,** 256, 120451. https://doi.org/10.1016/j.jclepro.2020.120451

[27] Sohani A, Shahverdian MH, Sayyaadi H, Samiezadeh S, Doranehgard MH, Nizetic S, Karimi N. Selecting the best nanofluid type for A photovoltaic thermal (PV/T) system based on reliability, efficiency, energy, economic, and environmental criteria. Journal of the Taiwan Institute of Chemical Engineers. **2021**, 124, 351-8. https://doi.org/10.1016/j.jtice.2021.02.027

[28] Deshmukh M, Satpute J, Purwant N, Deshmukh D, Chavhan S. Comparative analysis of CuO-based spiral flow photovoltaic sheet and tube thermal system. Thermal Science. **2022**, 26(2 Part C), 1747-55. https://doi.org/10.2298/TSCI201112197D

[29] Rosli MA, Rou CJ, Sanusi N, Saleem SN, Salimen N, Herawan SG, Abdullah N, Permanasari AA, Arifin Z, Hussain F. Numerical Investigation on Using MWCNT/Water Nanofluids in Photovoltaic Thermal System (PVT). Journal of Advanced Research in Fluid Mechanics and Thermal Sciences. **2022**, 99(1), 35-57. https://doi.org/10.37934/arfmts.99.1.3557

[30] Chaichan MT, Kazem HA, Alamiery AA, Isahak WN, Kadhum AA, Takriff MS. Adding nano-TiO2 to water and paraffin to enhance total efficiency of a photovoltaic thermal PV/T system subjected to harsh weathers. Nanomaterials. **2022**, 12(13), 2266. https://doi.org/10.3390/nano12132266

[31]   Prasetyo SD, Prabowo AR, Arifin Z. The use of a hybrid photovoltaic/thermal (PV/T) collector system as a sustainable energy-harvest instrument in urban technology. Heliyon. **2023,** 9(2), e13390. https://doi.org/10.1016/j.heliyon.2023.e13390

[32]   Prasad PD, Gupta AV. Experimental investigation on enhancement of heat transfer using Al2O3/water nanofluid in a u-tube with twisted tape inserts. International Communications in Heat and Mass Transfer. **2016**, 75, 154-61. https://doi.org/10.1016/j.icheatmasstransfer.2016.03.019

[33]   Sowi SA, Abdullah S, Sopian K. The effect of linearly increasing/decreasing pitch ratio twisted tape with various progression rate and nanofluid towards the system performance. Thermal Science and Engineering Progress. **2021**, 25, 100979. https://doi.org/10.1016/j.tsep.2021.100979

[34]   Mozaffari J, Mirjalily SA, Ahrar AJ. Experimental investigation of enhancing influence of Al2O3 nanoparticles on the convective heat transfer in a tube equipped with twisted tape inserts. Thermal Science. **2021,** 25(1 Part B), 541-51. https://doi.org/10.2298/TSCI181010414M

[35]   Afsharpanah F, Sheshpoli AZ, Pakzad K, Ajarostaghi SS. Numerical investigation of non-uniform heat transfer enhancement in parabolic trough solar collectors using dual modified twisted-tape inserts. Journal of Thermal Engineering. **2021** 7(1), 133-47. https://doi.org/10.18186/thermal.846584

[36]   Sheikholeslami M, Farshad SA. Investigation of solar collector system with turbulator considering hybrid nanoparticles. Renewable Energy. **2021**, 171, 1128-58. https://doi.org/10.1016/j.renene.2021.02.137

[37]   Gnanamuthu F, Anandan SS. Experimental Studies of Metal Oxide Suspended Nanofluids on the Enhancement of the Thermal Performance of Heat Pipes. Transactions of FAMENA. **2023**, 47(2):1-2. https://doi.org/10.21278/TOF.472046222

[38]   Al-Shamani AN, Yazdi MH, Alghoul MA, Abed AM, Ruslan MH, Mat S, Sopian K. Nanofluids for improved efficiency in cooling solar collectors–a review. Renewable and Sustainable Energy Reviews. **2014**, 38, 348-67. https://doi.org/10.1016/j.rser.2014.05.041

[39]   Karabulut, K. Investigation of heat transfer improvements of graphene oxide-water and diamond-water nanofluids in cross-flow-impinging jet flow channels having fin. *Isı Bilimi ve Tekniği Dergisi*, **2023** *43*(1), 11-30. doii..orrg//10..47480//iisiibtted.1290668

[40]   Karabulut, K. Heat transfer increment study taking into consideration fin lengths for CuO-water nanofluid in cross flow-impinging jet flow channels. *Thermal Science*, **2023**. (00), 35-35. https://doi.org/10.2298/TSCI221203035K

[41]   Kılınç F, Buyruk E, Karabulut K. Experimental investigation of cooling performance with graphene based nano-fluids in a vehicle radiator. Heat and Mass Transfer. **2020,** 56, 521–530. https://doi.org/10.1007/s00231-019-02722-x

[42]   Karabulut K, Buyruk E, Kilinc F. Experimental and numerical investigation of convection heat transfer in a circular copper tube using graphene oxide nanofluid. Journal of the Brazilian Society of Mechanical Sciences and Engineering. **2020**, 42(5):230. https://doi.org/10.1007/s40430-020-02319-0

[43]   Karabulut KO, Alnak DE. Investigation of graphene oxide-distilled water nanofluids with consideration of heat transfer and flow structure for backward-facing step flow. Journal of Engineering Thermophysics. **2021**; 30, 300–316. https://doi.org/10.1134/S1810232821020119

[44]   Shen C, Zhang Y, Zhang C, Pu J, Wei S, Dong Y. A numerical investigation on optimization of PV/T systems with the field synergy theory. Applied Thermal Engineering. **2021**, 185, 116381. https://doi.org/10.1016/j.applthermaleng.2020.116381

[45]   Jiji LM, Jiji LM. Heat convection. Berlin: Springer; **2006**, 434. https://doi.org/10.1007/978-3-540-30694-8

[46]   Nfawa SR, Basri AA, Masuri SU. Novel use of MgO nanoparticle additive for enhancing the thermal conductivity of CuO/water nanofluid. Case Studies in Thermal Engineering. **2021,** 27, 101279. https://doi.org/10.1016/j.csite.2021.101279

[47]   Ghadikolaei SS, Hosseinzadeh K, Hatami M, Ganji DD. MHD boundary layer analysis for micropolar dusty fluid containing Hybrid nanoparticles (Cu-Al2O3) over a porous medium. Journal of Molecular Liquids. **2018**, 268, 813-23. https://doi.org/10.1016/j.molliq.2018.07.105

[48]   Adam NM, Attia OH, Al-Sulttani AO, Mahmood HA, As'arry A, Rezali KA. Numerical Analysis for Solar Panel Subjected with an External Force to Overcome Adhesive Force in Desert Areas. CFD Letters. **2020**, 12(9), 60-75. https://doi.org/10.37934/cfdl.12.9.6075

Saleh Mutashar Hussein*
Assoc. Prof. Moharram Jafari
Prof. Mohammad Taghi Shervani-Tabar
Prof. Seyed Esmail Razavi
Department of Mechanical Engineering,
University of Tabriz, Tabriz, Iran
*Corresponding author:
saleh75.hussein@gmail.com